THE JOURNAL OF PHYSICAL CHEMISTRY Letters

LETTER

pubs.acs.org/JPCL

Patterning Vertically Oriented Graphene Sheets for Nanodevice Applications

Kehan Yu, Pengxiang Wang, Ganhua Lu, Ke-Hung Chen, Zheng Bo, and Junhong Chen*

Department of Mechanical Engineering, University of Wisconsin-Milwaukee, Milwaukee, Wisconsin 53201, United States

Supporting Information

ABSTRACT: Graphene has attracted growing interest in the past few years. Growing vertically oriented graphene sheets with a designed pattern is practically attractive for device applications based on graphene. Here we report a patterned synthesis of vertical graphene nanosheets using plasma-enhanced chemical vapor deposition. Both experimental and modeling results suggest that the electric field distribution above the substrate material plays a key role in the graphene coverage. Vertical graphene patterns can thus be designed through artificially designing the surface electric field distribution. A field-effect transistor (FET) sensor device has been demonstrated for detection of low-concentration gases using vertically patterned graphene sheets bridging a metal electrode gap.

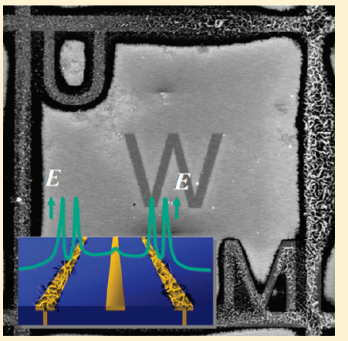

SECTION: Nanoparticles and Nanostructures

Graphene has been actively explored as potential building blocks for various electronic device applications, as they offer unique mechanical, electrical, and chemical properties arising from their carbon constituents and very small dimensions.[1−6] For example, they may assist the further scaling down of devices into the molecular regime, enabling enhanced performance and new functionality, leading to novel technological applications. For instance, graphene has been demonstrated for numerous applications such as in electronic devices, energy storage, solar cells, chemical/biological sensors, display devices, catalysis, and ultrafast photodetectors.[7−16] In order to build integrated devices and systems for nanoelectronic applications, nanoscale structures often need to be arranged into well-defined configurations. Existing methods for patterning horizontal graphene include catalyst patterns during growth,[17−19] mask lithography,[20,21] transfer printing,[22,23] and direct-write processes.[24−26] Methods to grow vertical graphene patterns are scarce, and the control mechanism is not understood. Only a few studies on selective growth of vertical graphene by means of patterned catalysts or deep trenches have been reported.[27,28]

We have recently demonstrated an atmospheric glow discharge method to grow vertically oriented graphene sheets or carbon nanowalls (CNWs).[29,30] These two-dimensional (2D) "graphitic" platelets typically oriented vertically on a substrate were reported to have a few stacked layers (graphitic) with typical lateral dimensions of several micrometers.[30,31] The sharp edges and vertical orientation make CNWs a potential field emission material.[32−34] The high surface area of CNWs means they are of interest as a potential catalyst support. For instance, CNWs have been tested for use in Li-ion batteries[35] and electrochemical capacitors.[36] In this letter, we report on patterned synthesis of CNWs with a direct current (dc) plasma-enhanced chemical vapor deposition (PECVD) system at atmospheric pressure through designing the surface electric field distribution. We further understand the pattern growth mechanism through combining experiments with numerical simulations. Finally, we demonstrate a field-effect transistor (FET) device based on these CNW patterns for detection of low-concentration gases. The pattern growth method presented here provides a new perspective for graphene-based nanoelectronic applications.

Specifically, the growth substrate (oxidized Si wafer) was first patterned and then sputter-coated with gold electrodes of 1−5 μm wide. The configuration of the plasma reactor used for the CNW growth is illustrated in Figure 1. A tungsten pin cathode pointing toward the substrate carrying −2 kV was placed 1 cm away from the substrate. The gold pattern included a network of squares and the letters U, W, and M. The letters U and M were connected to the square network, while the letter W was isolated. During the CNW growth, the gold network that includes the squares and letters U and M was grounded, whereas the letter W was floating.

High-resolution transmission electron microscopy (HRTEM) images of the product CNWs are shown in Figure 1(b,c), which confirms that the CNW sheets consist of a few graphene layers (typically about 10 layers, Figure 1b). The edges of the suspended CNWs often fold back, allowing for a cross-sectional view of the graphene.[37] By observing these edges through HRTEM images, the number of layers at multiple locations on the graphene can be measured (indicated by a red line in Figure 1b). The estimated interlayer spacing is about 3.41 ± 0.02 Å, which is a little larger than the *d*-spacing of graphite (3.36 Å) (Figure 1c). The small amount of oxygen-containing functional groups induced by the trace amount of water vapor used in

Received: January 19, 2011
Accepted: February 9, 2011
Published: February 21, 2011

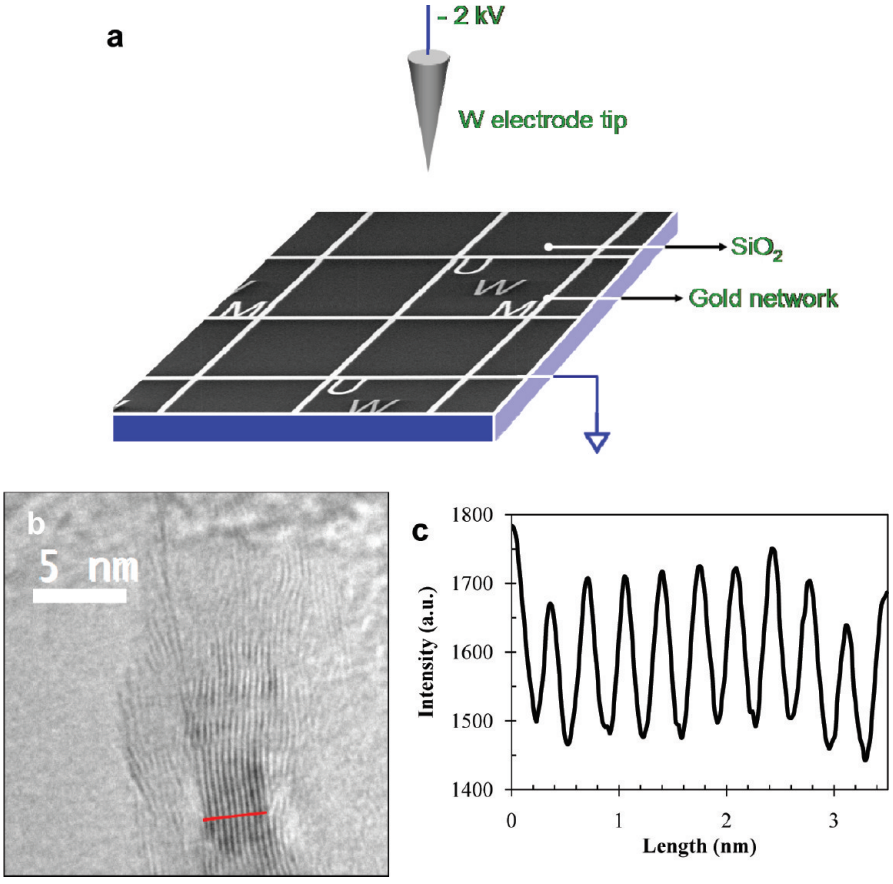

Figure 1. (a) Experimental setup for PECVD growth of CNWs. A gold pattern including a network of squares and letters U, W, and M was coated on the SiO_2 substrate. (b,c) TEM characterization of CNWs. (b) HRTEM image of a multilayer CNW showing parallel graphene sheets. The number of walls is about 10. (c) The intensity profile corresponding to the red line in panel b. The spacing of interlayer graphene sheets in the CNW is measured as 3.41 ± 0.02 Å based on the intensity profile (c).

the carrier gas might be responsible for this difference.[38] We note that the interlayer spacing is slightly smaller than that of our earlier work, in which more water vapor (feed gas relative humidity 39.3%) was introduced.[29] The graphitic structure of CNWs grown using CH_4 or C_2H_2 was confirmed by Raman spectra of resulting CNW samples, which clearly exhibit a significant 2D band (Supporting Information, Figure S1).

Scanning electron microscopy (SEM) images in Figure 2 showing CNWs grown on the patterned SiO_2/Si substrate clearly suggest that CNWs can be selectively grown on grounded metal electrodes in contrast to the floating metal electrode surface and the dielectric surface. Figure 2a shows an overview of the patterned CNW growth. A close view of the substrate shows that CNWs grew on the grounded square network and letters (Figure 2b). In particular, CNWs were grown on M and U electrodes with a clear contrast between the grounded gold electrode and the SiO_2 surface (Figure 2c,d). An enlarged view of CNWs reveals the vertical orientation of the graphene sheets (Figure 2e). The lateral dimension of most graphene sheets was greater than 1 μm. On the other hand, no CNW was found on the isolated W letter electrode and the dielectric SiO_2 surface (Figure 2f).

It can be inferred that the growth of CNWs is closely related to the electric field distribution near the substrate surface. To further understand the preferential growth of CNWs on the grounded gold electrode, we computed distributions of electrical potential and electric field in the space near the substrate for three cases (shown in Figure 3). A tungsten pin carrying −2 kV was placed 1 cm away from the substrate (defined as $X-Y$ plane). Infinitely long gold stripes (1 μm in width) lying on the SiO_2 substrate were grounded ($V = 0$). The positions of gold stripes are illustrated in Figure 3a, c, and e as yellow stripes, as well as in Supporting Information Scheme S1. In case I, one single stripe is placed between $x = -0.5$ μm and $x = 0.5$ μm. In case II, two parallel stripes are placed on the substrate: one grounded stripe is placed between $x = -0.5$ μm and $x = 0.5$ μm, and the other isolated stripe is placed between $x = 1.5$ μm and $x = 2.5$ μm. In case III, three parallel stripes are placed on the substrate: The first and the second are grounded and placed between $x = -0.5$ μm and $x = 0.5$ μm and $x = 4.5$ μm and $x = 5.5$ μm, respectively. The third is placed between $x = 2$ μm and $x = 3$ μm, which is isolated. Although the tungsten tip is sharp, it is still much larger than the width of the gold stripe (1 μm). In the computational model, we treated the tungsten tip as an infinite and flat equipotential body.

Figure 3 shows modeling results of electric field near the substrate and corresponding experimental results. The results of electric potential are available in the Supporting Information (Figure S2). The electric field at 50 nm above the substrate of case I is displayed in Figure 3a. The electric field above the gold stripe especially near the edges (with even smaller radii of curvature) of the gold stripe is much larger than that above the SiO_2. As a result, the gas was ionized more efficiently above the gold stripe during the growth process so that CNWs can be found

dx.doi.org/10.1021/jz200087w |J. Phys. Chem. Lett. 2011, 2, 537–542

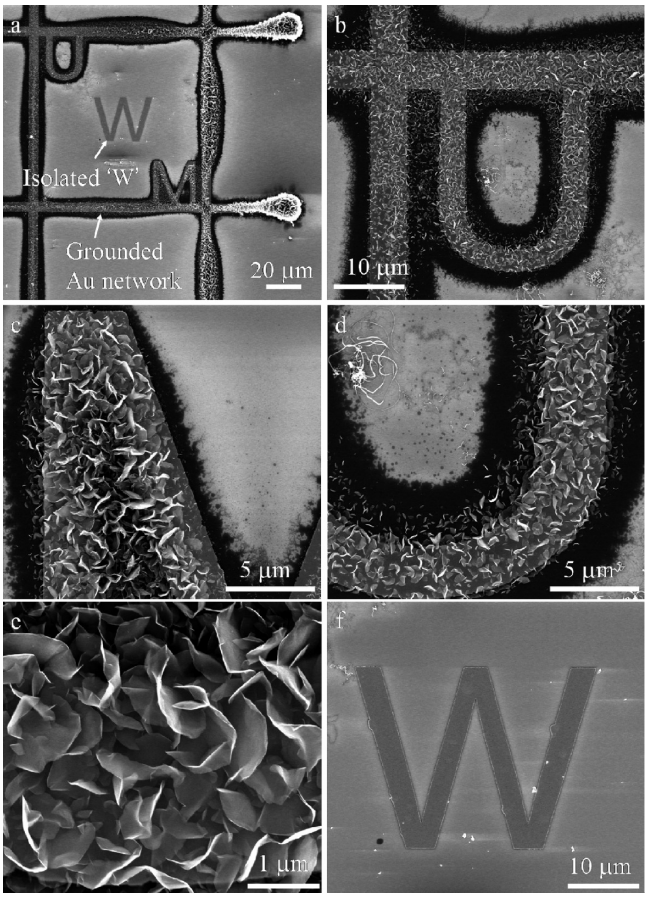

Figure 2. SEM images of patterned CNWs. (a) An overview of the CNW distribution on the patterned substrate with a grounded gold square network and the letters U and M. (b) A close view showing CNWs grown on the grounded network and the letter U. (c,d) CNWs were grown on letters M and U, respectively. The clear boundaries distinguish gold from SiO_2. (e) Enlarged view of CNWs showing vertical orientation of graphene nanosheets. Lateral dimensions of most graphene sheets are larger than 1 μm. (f) No CNW growth was found on the isolated letter W.

immediately on the Au surface after the introduction of carbon precursors (Figure 3b, 2 min of growth). In contrast, neither CNWs nor amorphous carbon was found on the SiO_2 for up to 10 min of the growth with the help of SEM and Raman spectroscopy analysis. Figure 3c displays an electric field at 50 nm above the substrate of case II. The overall electric field above the grounded gold stripe is larger than that above the isolated gold stripe. Similarly, the right edge (x = 2.5 μm) of the isolated stripe has a relatively high electric field. However, the electric field at the left edge (x = 1.5 μm) is much lower. The variation of the electric field above the isolated stripe is caused by the screening effect induced by the nearby grounded stripe. The corresponding experimental result is shown in Figure 3d. The CNWs were grown on both stripes due to the electric field distribution. The CNWs spread off the left edge of the grounded stripe, while the growth was cut off at the right edge of the isolated stripe. The asymmetric growth was consistent with the electric field distribution, i.e., the field above the edge of the isolated stripe is lower than that of the grounded stripe. Figure 3e displays an electric field at 50 nm above the substrate of case III. Compared with the electric field distribution in case II, both edges of the isolated stripe were greatly affected by the screening effect. The highest electric field value above the isolated stripe is only about 1/7 of that of the grounded stripe. The corresponding experiment is the CNW growth on the UWM logo. We conclude that the absence of CNWs on the W is attributed to the aforementioned screening effect.

Given the surface electric field-dominant growth mechanism, CNWs themselves could play a role as growth sites. CNWs grown on single Au stripes (1.0 μm in width) were examined with durations of 1 min, 2 min, 5 min, and 10 min (SEM images available in the Supporting Information, Figure S3). The width of the CNW growth region was about 1.0, 1.2, 7.2, and 8.0 μm, respectively, while the width of Au stripe is only 1 μm. It is likely that CNWs can be grown on the pregrown CNWs. Since CNWs can not be grown on the SiO_2 surface in the dc PECVD process, the only possibility is that the CNWs extended beyond the original Au stripe were grown on the pregrown CNWs due to the relatively higher electric field above these CNWs. Malesevic and co-workers also suggested that nucleation sites could form on the CNWs.[39] The electric field-selective growth of CNWs provides an effective route to patterned CNWs. In order to achieve a better spatial resolution, the synthesis parameters such as the growth time, should be deliberately optimized to confine the CNWs in the region of the original conductive pattern.

By taking advantage of the field-selective and the expanding growth of the CNWs, three-terminal gas sensing FETs were fabricated using resulting CNWs as the conducting channel. A pair of parallel Au electrodes with spacing of 1 μm were fabricated by an e-beam lithography process on silicon wafers with a 300 nm thick SiO_2 dielectric layer.[40] The growth duration was 2 min as it was found that this exposure would yield a film of CNWs connecting with two neighboring electrodes (Figure 3d). We made 18 good sensors out of total 20 samples, which suggests decent reliability of the simple fabrication method. The sensor was operated at room temperature and was exposed to clean dry air flow of 2 lpm for 10 min to record a base value of the sensor conductance, NO_2 (100 ppm) or NH_3 (1%) was diluted in air of 2 lpm for 15 min to register a sensing signal, and then a lab air flow of 2 lpm was used again for 25 min to recover the device. A constant current (100 nA) was applied across two gold terminals, and the voltage was monitored.

Upon exposure to NH_3 (1%), the sensor voltage went up, i.e., the resistance of the sensor increased (Figure 4a, violet curve). Upon the introduction of NO_2 (100 ppm), the sensor voltage went down (i.e., the resistance of the sensor decreased), as shown in Figure 4a (green curve). The sensor sensitivities are evaluated as the ratios of R_{air}/R_{NO2} for NO_2 and R_{NH3}/R_{air} for NH_3, where R_{air}, R_{NO2}, and R_{NH3} are the sensor resistances in clean air, air containing 100 ppm NO_2, and air containing 1% NH_3, respectively. The sensitivities to NO_2 and NH_3 are 1.57 and 1.13, respectively. Although the CNWs are not single-layer graphene, their sensitivities to NO_2 and NH_3 are comparable with those based on thermally reduced graphene oxide we reported previously.[40]

The CNW film behaves like a p-type semiconductor, similar to graphene when exposed to an ambient environment. The p-type nature of the CNWs in ambient condition was confirmed by the FET transport characteristics. The decreasing drain-source current as a function of increasing back-gate voltage shows a sign of p-type CNWs as the conducting channel (Figure 4b). The adsorbed NH_3 molecules donate electrons to CNWs and neutralize holes partially in the CNW, which results in a lower sensor current in the device. Likewise, NO_2 is a strong oxidizer with

dx.doi.org/10.1021/jz200087w |J. Phys. Chem. Lett. 2011, 2, 537–542

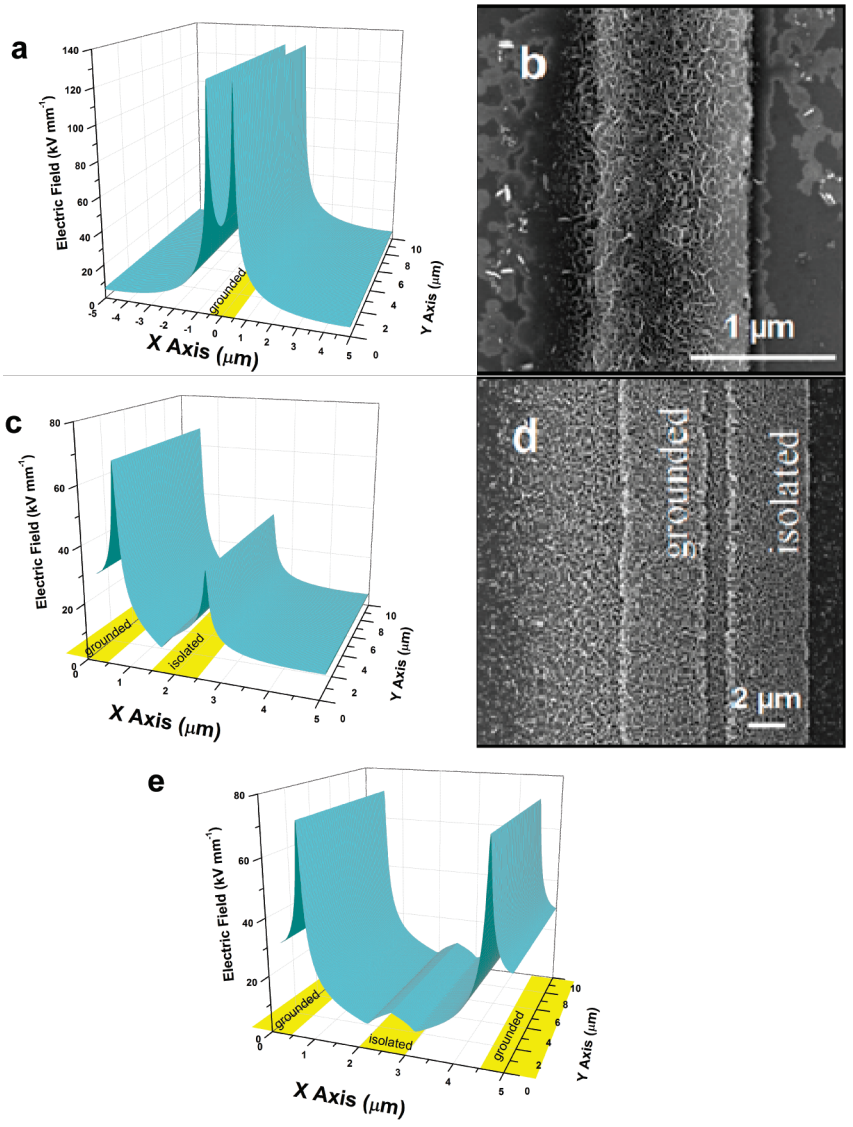

Figure 3. Modeling results of the electric field at 50 nm above the growth substrate and corresponding SEM images of CNWs (a,b, - case I; c,d - case II; e - case III). A tungsten tip carrying −2 kV was placed 1 cm away from the substrate. (a) Electric field distribution at 50 nm above the substrate surface of case I. The 1 μm-wide gold stripe is grounded ($V = 0$). (b) CNWs grown on the single gold stripe in 2 min. (c) Electric field at 50 nm above the substrate of case II. (d) CNWs grown on the parallel gold stripes in 2 min (note: the strip width here is 5 μm). (e) Electric field at 50 nm above the substrate of case III. The yellow stripes in the $X-Y$ plane illustrate locations of isolated or grounded gold stripes (assuming uniform distribution along the Y-direction).

electron-withdrawing power;[41] therefore, electron transfer from CNWs to adsorbed NO_2 leads to increased hole concentration and enhanced electrical conduction in the CNW network. The sensing behavior of the as-grown CNW is consistent with a typical graphene-based gas sensor.[40] Similar to gas sensors based on CNTs[42] and graphene,[40] slow recovery was observed for CNW sensors. The thermal energy at room temperature is typically insufficient to overcome the activation energy needed for molecule desorption.[43]

In summary, patterned growth of vertically oriented graphene sheets or CNWs was achieved through strategically patterning gold electrodes on the SiO_2 surface. CNWs were successfully grown on grounded, microfabricated straight gold stripes and gold UWM logos. In contrast, no CNWs were grown on the surface of the dielectric SiO_2 or floating gold surface. Both experimental and modeling results suggest that the electric field distribution above the substrate material plays a key role on the CNW coverage. Additionally, the electric field distribution was strongly affected by the field screening effect. A reliable gas sensing FET fabrication was demonstrated with the electric-field induced patterning growth. The CNWs exhibit p-type semiconducting properties in ambient conditions and sensitivity to low-concentration NO_2 and NH_3.

EXPERIMENTAL SECTION

The growth substrate (oxidized Si wafer with SiO_2 of 300 nm in thick) was first patterned using e-beam lithography (JEOL 9300F e-beam lithography tool, 100 kV) and then sputter-coated with gold electrodes of 50 nm thickness. In order to more precisely control the carbon source in the reaction atmosphere, Ar and CH_4 (or C_2H_2) flows were introduced into the reactor with two separate mass flow controllers. An Ar/CH_4 flow (10% CH_4 by volume, 1000 sccm) or an Ar/C_2H_2 flow (5% C_2H_2 by

dx.doi.org/10.1021/jz200087w |J. Phys. Chem. Lett. 2011, 2, 537–542

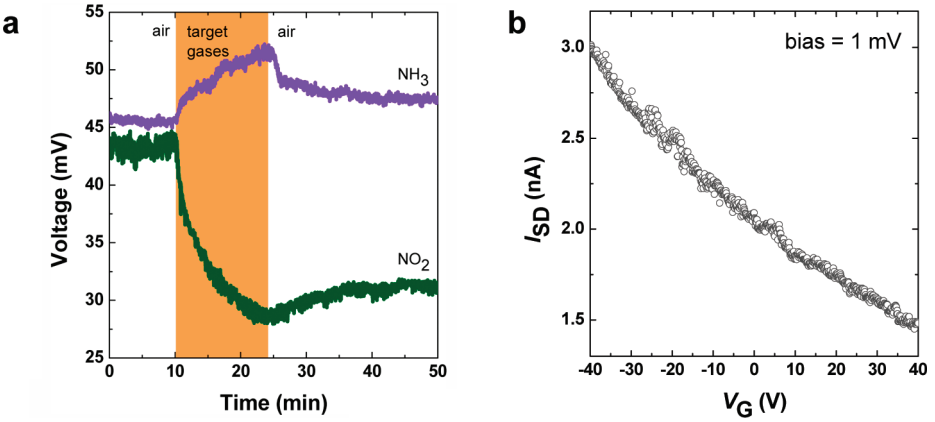

Figure 4. (a) Room-temperature sensing response for NO_2 (100 ppm) and NH_3 (1%). (b) The transport characteristic of a three-terminal CNW FET.

volume, 1000 sccm) together with a small amount of water vapor (CH_4 or C_2H_2 flow through a bubbler) was used. The relative humidity of the running feed gas was ~5.1% before reaching the PECVD reactor. Our experiments suggest that acetylene can be dissociated at a lower temperature and lead to larger graphene nanosheets. Growth duration varied from 30 s to 10 min. It took 5 min for CNWs to grow on the UWM logo (Figure 2). For the sensing device, a growth period of 30 s to 2 min was preferred. The CNW growth rate on a narrower conductor line was faster, so a short growth period can be used to confine CNWs precisely within the conductor pattern. To avoid damage to the gold pattern by Ar ion bombardment, the Ar carrier gas can be replaced with H_2, especially for a long growth period. No catalysts were used throughout the CNW growth.

TEM analysis of CNWs was carried out using a Hitachi H 9000 NAR TEM with a point resolution of 0.18 nm at 300 kV in the phase contrast HRTEM imaging mode. TEM samples were prepared by growing CNWs on Cu TEM grids directly. The morphology of resulting CNWs on substrates was characterized using a field-emission SEM (Hitachi S 4800), which has a resolution of 1.4 nm at 1 kV acceleration voltage. Both transport characteristics ($I_{SD}-V_G$) and gas sensing performance of the CNW FET device were measured using a Keithley 2602 source meter.

■ ASSOCIATED CONTENT

Supporting Information. Figure S1, Raman spectra of CNWs. Figure S2, electrical potential profiles above substrates of cases I, II, and III. Figure S3, SEM images of time-dependent growth of CNWs. Scheme S1, locations of gold stripes in the $X-Y$ plane for cases I, II, and III. This material is available free of charge via the Internet at http://pubs.acs.org.

■ AUTHOR INFORMATION

Corresponding Author
*E-mail: jhchen@uwm.edu.

■ ACKNOWLEDGMENT

This work was financially supported by the NSF (CMMI-0900509), DOE (DE-EE0003208), and We Energies. SEM, TEM, and electrode fabrication were performed in the UWM Electron Microscope Laboratory, UWM HRTEM Laboratory, and Argonne National Laboratory, respectively.

■ REFERENCES

(1) Geim, A. K.; Novoselov, K. S. The Rise of Graphene. *Nat. Mater.* **2007**, *6*, 183–191.
(2) Dreyer, D. R.; Park, S.; Bielawski, C. W.; Ruoff, R. S. The Chemistry of Graphene Oxide. *Chem. Soc. Rev.* **2010**, *39*, 228–240.
(3) Dreyer, D. R.; Ruoff, R. S.; Bielawski, C. W. From Conception to Realization: An Historial Account of Graphene and Some Perspectives for Its Future. *Angew. Chem., Int. Ed.* **2010**, *49*, 9336–9344.
(4) Rao, C. N. R.; Sood, A. K.; Voggu, R.; Subrahmanyam, K. S. Some Novel Attributes of Graphene. *J. Phys. Chem. Lett.* **2010**, *1*, 572–580.
(5) Green, A. A.; Hersam, M. C. Emerging Methods for Producing Monodisperse Graphene Dispersions. *J. Phys. Chem. Lett.* **2010**, *1*, 544–549.
(6) Li, L.-s.; Yan, X. Colloidal Graphene Quantum Dots. *J. Phys. Chem. Lett.* **2010**, *1*, 2572–2576.
(7) Potts, J. R.; Dreyer, D. R.; Bielawski, C. W.; Ruoff, R. S. Graphene-Based Polymer Nanocomposites. *Polymer* **2011**, *52*, 5–25.
(8) Schedin, F.; Geim, A. K.; Morozov, S. V.; Hill, E. W.; Blake, P.; Katsnelson, M. I.; Novoselov, K. S. Detection of Individual Gas Molecules Adsorbed on Graphene. *Nat. Mater.* **2007**, *6*, 652–655.
(9) Wang, X.; Ouyang, Y.; Li, X.; Wang, H.; Guo, J.; Dai, H. Room-Temperature All-Semiconducting Sub-10-nm Graphene Nanoribbon Field-Effect Transistors. *Phys. Rev. Lett.* **2008**, *100*, 206803–206806.
(10) Xia, F.; Mueller, T.; Lin, Y.-m.; Valdes-Garcia, A.; Avouris, P. Ultrafast Graphene Photodetector. *Nat. Nanotechnol.* **2009**, *4*, 839–843.
(11) Blake, P.; Brimicombe, P. D.; Nair, R. R.; Booth, T. J.; Jiang, D.; Schedin, F.; Ponomarenko, L. A.; Morozov, S. V.; Gleeson, H. F.; Hill, E. W.; et al. Graphene-Based Liquid Crystal Device. *Nano Lett.* **2008**, *8*, 1704–1708.
(12) Tylianakis, E.; Psofogiannakis, G. M.; Froudakis, G. E. Li-Doped Pillared Graphene Oxide: A Graphene-Based Nanostructured Material for Hydrogen Storage. *J. Phys. Chem. Lett.* **2010**, *1*, 2459–2464.
(13) Ng, Y. H.; Lightcap, I. V.; Goodwin, K.; Matsumura, M.; Kamat, P. V. To What Extent Do Graphene Scaffolds Improve the Photovoltaic and Photocatalytic Response of TiO_2 Nanostructured Films?. *J. Phys. Chem. Lett.* **2010**, *1*, 2222–2227.
(14) Kim, T. Y.; Lee, H. W.; Stoller, M.; Dreyer, D. R.; Bielawski, C. W.; Ruoff, R. S.; Suh, K. S. High-Performance Supercapacitors Based on Poly(ionic liquid)-Modified Graphene Electrodes. *ACS Nano* **2011**, *5*, 436–442.
(15) Dreyer, D. R.; Jia, H.-P.; Bielawski, C. W. Graphene Oxide: A Convenient Carbocatalyst for Facilitating Oxidation and Hydration Reactions. *Angew. Chem., Int. Ed.* **2010**, *49*, 6813–6816.

(16) Kamat, P. V. Graphene-Based Nanoarchitectures. Anchoring Semiconductor and Metal Nanoparticles on a Two-Dimensional Carbon Support. *J. Phys. Chem. Lett.* **2010**, *1*, 520–527.
(17) Di, C.; Wei, D.; Yu, G.; Liu, Y.; Guo, Y.; Zhu, D. Patterned Graphene as Source/Drain Electrodes for Bottom-Contact Organic Field-Effect Transistors. *Adv. Mater.* **2008**, *20*, 3289–3293.
(18) Reina, A.; Jia, X.; Ho, J.; Nezich, D.; Son, H.; Bulovic, V.; Dresselhaus, M. S.; Kong, J. Large Area, Few-Layer Graphene Films on Arbitrary Substrates by Chemical Vapor Deposition. *Nano Lett.* **2008**, *9*, 30–35.
(19) Kim, K. S.; Zhao, Y.; Jang, H.; Lee, S. Y.; Kim, J. M.; Kim, K. S.; Ahn, J.-H.; Kim, P.; Choi, J.-Y.; Hong, B. H. Large-Scale Pattern Growth of Graphene Films for Stretchable Transparent Electrodes. *Nature* **2009**, *457*, 706–710.
(20) Chen, Z.; Lin, Y.-M.; Rooks, M. J.; Avouris, P. Graphene Nano-ribbon Electronics. *Physica E* **2007**, *40*, 228–232.
(21) Bai, J.; Duan, X.; Huang, Y. Rational Fabrication of Graphene Nanoribbons Using a Nanowire Etch Mask. *Nano Lett.* **2009**, *9*, 2083–2087.
(22) Song, L.; Ci, L.; Gao, W.; Ajayan, P. M. Transfer Printing of Graphene Using Gold Film. *ACS Nano* **2009**, *3*, 1353–1356.
(23) Allen, M. J.; Tung, V. C.; Gomez, L.; Xu, Z.; Chen, L. M.; Nelson, K. S.; Zhou, C.; Kaner, R. B.; Yang, Y. Soft Transfer Printing of Chemically Converted Graphene. *Adv. Mater.* **2009**, *21*, 2098–2102.
(24) Tapaszto, L.; Dobrik, G.; Lambin, P.; Biro, L. P. Tailoring the Atomic Structure of Graphene Nanoribbons by Scanning Tunnelling Microscope Lithography. *Nat. Nanotechnol.* **2008**, *3*, 397–401.
(25) Lemme, M. C.; Bell, D. C.; Williams, J. R.; Stern, L. A.; Baugher, B. W. H.; Jarillo-Herrero, P.; Marcus, C. M. Etching of Graphene Devices with a Helium Ion Beam. *ACS Nano* **2009**, *3*, 2674–2676.
(26) Fischbein, M. D.; Drndic, M. Electron Beam Nanosculpting of Suspended Graphene Sheets. *Appl. Phys. Lett.* **2008**, *93*, 113107–113109.
(27) Wu, Y. H.; Yang, B. J.; Han, G. C.; Zong, B. Y.; Ni, H. Q.; Luo, P.; Chong, T. C.; Low, T. S.; Shen, Z. X. Fabrication of a Class of Nanostructured Materials Using Carbon Nanowalls as the Templates. *Adv. Funct. Mater.* **2002**, *12*, 489–494.
(28) Hiramatsu, M.; Hori, M. *Carbon Nanowalls: Synthesis and Emerging Applications*; Springer: New York, 2010.
(29) Bo, Z.; Yu, K.; Lu, G.; Wang, P.; Mao, S.; Chen, J. Understanding Growth of Carbon Nanowalls at Atmospheric Pressure Using Normal Glow Discharge Plasma-Enhanced Chemical Vapor Deposition. *Carbon* **2011**No. 10.1016/j.carbon.2011.01.007.
(30) Yu, K.; Bo, Z.; Lu, G.; Mao, S.; Cui, S.; Zhu, Y.; Chen, X.; Ruoff, R. S.; Chen, J. Growth of Carbon Nanowalls at Atmospheric Pressure for One-Step Gas Sensor Fabrication. *Nanoscale Res. Lett.* **2011**in press.
(31) Malesevic, A.; Kemps, R.; Vanhulsel, A.; Chowdhury, M. P.; Volodin, A.; Van Haesendonck, C. Field Emission from Vertically Aligned Few-Layer Graphene. *J. Appl. Phys.* **2008**, *104*, 084301–084305.
(32) Watcharotone, S.; Ruoff, R. S.; Read, F. H. Possibilities for Graphene for Field Emission: Modeling Studies Using the BEM. *Phys. Procedia* **2008**, *1*, 71–75.
(33) Hiraki, H.; Jiang, N.; Wang, H. X.; Hiraki, A. Electron Emission from Nano-Structured Carbon Composite Materials - An Important Role of the Interface for Enhancing the Emission. *J. Phys. IV* **2006**, *132*, 111–115.
(34) Takyo, G.; Kono, S.; Goto, T.; Sasaoka, H.; Nishimura, K. Origin of Field Emission from a Nano-diamond/Carbon Nanowall Electron Emitter. *Jpn. J. Appl. Phys.* **2008**, *47*, 2241–2243.
(35) Tanaike, O.; Kitada, N.; Yoshimura, H.; Hatori, H.; Kojima, K.; Tachibana, M. Lithium Insertion Behavior of Carbon Nanowalls by dc Plasma CVD and Its Heat-Treatment Effect. *Solid State Ionics* **2009**, *180*, 381–385.
(36) Hung, T. C.; Chen, C. F.; Whang, W. T. Deposition of Carbon Nanowall Flowers on Two-Dimensional Sheet for Electrochemical Capacitor Application. *Electrochem. Solid State Lett.* **2009**, *12*, K41–K44.
(37) Reina, A.; Jia, X. T.; Ho, J.; Nezich, D.; Son, H. B.; Bulovic, V.; Dresselhaus, M. S.; Kong, J. Large Area, Few-Layer Graphene Films on Arbitrary Substrates by Chemical Vapor Deposition. *Nano Lett.* **2009**, *9*, 30–35.
(38) Gao, W.; Alemany, L. B.; Ci, L.; Ajayan, P. M. New Insights into the Structure and Reduction of Graphite Oxide. *Nat. Chem.* **2009**, *1*, 403–408.
(39) Malesevic, A.; Vitchev, R.; Schouteden, K.; Volodin, A.; Zhang, L.; Van Tendeloo, G.; Vanhulsel, A.; Van Haesendonck, C. Synthesis of Few-Layer Graphene via Microwave Plasma-Enhanced Chemical Vapour Deposition. *Nanotechnology* **2008**, *19*, 305604–305609.
(40) Lu, G.; Ocola, L. E.; Chen, J. Gas Detection Using Low-Temperature Reduced Graphene Oxide Sheets. *Appl. Phys. Lett.* **2009**, *94*, 083111–083113.
(41) Leenaerts, O.; Partoens, B.; Peeters, F. M. Adsorption of H_2O, NH_3, CO, NO_2, and NO on Graphene: A First-Principles Study. *Phys. Rev. B* **2008**, *77*, 125416–125421.
(42) Kong, J.; Franklin, N. R.; Zhou, C.; Chapline, M. G.; Peng, S.; Cho, K.; Dai, H. Nanotube Molecular Wires as Chemical Sensors. *Science* **2000**, *287*, 622–625.
(43) Fan, Z.; Lu, J. G. Gate-Refreshable Nanowire Chemical Sensors. *Appl. Phys. Lett.* **2005**, *86*, 123510–123512.